Measurement of production cross sections of the Higgs boson in the four-lepton final state in proton-proton collisions at $\sqrt{s} = 13$ TeV

The CMS Collaboration

Friday, 2021-06-11

For the discussion of science...

Romal Kumar

Outline

Introduction

- $H \rightarrow ZZ \rightarrow 4\,l$ decay – large signal-to-background
- Measurements from this decay channel: mass, spin, and parity of H boson, width, and the inclusive and differential fiducial cross section
- Data analysis performed on LHC Run–2 data by the CMS detector. With integrated luminosities of 35.9, 41.5, and 59.7 fb^{-1} in the years 2016, 2017, and 2018. Total integrated luminosity of 137 fb^{-1}
- Measurement of the H boson cross section within the Simplified Template Cross Section (STXS) framework; implements stage 1.2 bins in $H \rightarrow 4\,l$ decay channel

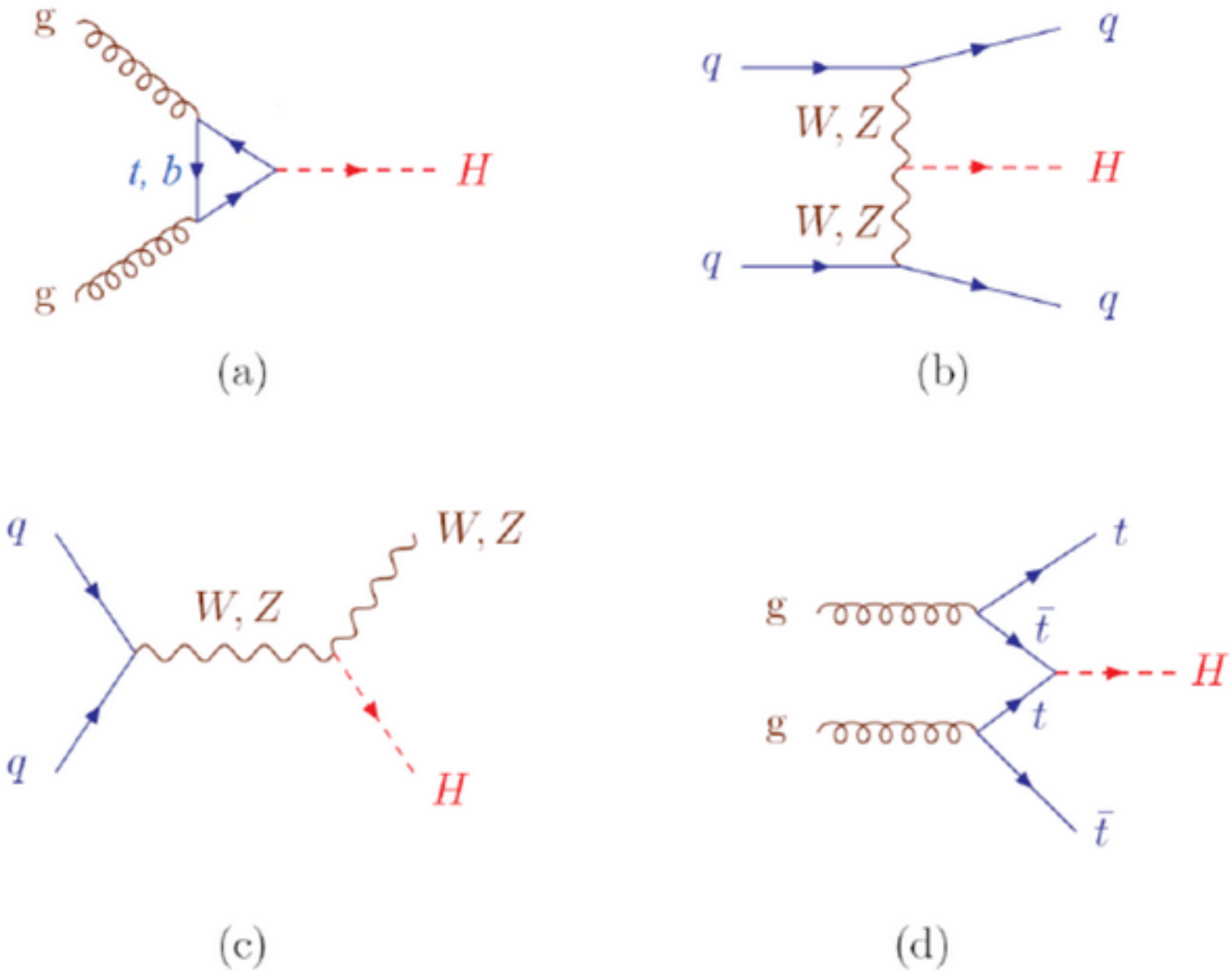

Figure 1: Higgs production channels: (a)gluon-gluon fusion, ggH (b)Vector Boson Fusion, VBF (c)Vector-Higgs, VH (WH or ZH) (d)t $\bar{t}$ H

CMS detector

General

- Superconducting solenoid of $6\,m$ internal diameter providing a magnetic field of $3.8\,\mathrm{T}$
- Silicon pixel and strip tracker
- Lead tungstate crystal in ECAL
- Brass and scintillator HCAL
- Forward calorimeters extend the pseudorapidity η coverage
- Muons detected in gas-ionization chambers outside the solenoid

Data acquisition

- Events of interest selected using a two-tiered trigger system
- First level selects events around 100 kHz rate
- Second level (high-level trigger) reduces event rate to 1 kHz before data storage

On measurement

- Momentum resolution for electrons ranges from 1.7% to 4.5%
- Muons measured in the pseudorapidity range $|\eta| < 2.4$
- Efficiency to reconstruct and identify muons exceed 96%

Event reconstruction and selection

- Particle-flow algorithm to reconstruct and identify each individual particle, optimized combination from various elements of the CMS detector
- An isolation requirement of $\mathcal{I}^{\mu} < 0.35$ to discriminate between prompt muons from Z decay and those arising from electroweak decay in jets
- Electrons are identified using a multivariate discriminant analysis
- Hadronic jets reconstructed using infrared and collinear-safe anti-k_T algorithm
- Tracks identified originating from pileup vertices are discarded and an offset correction is applied

$$\mathcal{I} \equiv \sum p_T^{\text{charged}} + \max[0, \sum p_T^{\text{neutral}} + \sum p_T^{\gamma} - p_T^{\mu,\text{PU}}]/p_T^{\mu}$$

A good rule of thumb to remember

Jet energy resolution amounts typically to 16% at 30 GeV, 8% at 100 GeV, and 4% at 1 TeV

- Event selection designed to extract signal candidates from events containing at least four well-identified and isolated leptons
- ZZ candidates ($12 < m_{l^+l^-} < 120$ GeV) as:
  - Z_1 with an invariant mass close to the nominal Z boson
  - Z_2 as the other one

Finally

Events are further selected based on kinematic discriminants and then categorized based on STXS frameworks

Event categorization

- Organized in two steps with increasing granularity of the categories
- Step 1: separate ggH, VBF, VH, and $\mathrm{t}\bar{t}\mathrm{H}$ processes
- Step 2: subdivision of the above category using recommended binning of STXS framework

STXS stands for Standard Template Cross Section. It is adopted by LHC experiments as a common framework for Higgs measurements.

STXS framework

- To reduce the theoretical uncertainties that are directly folded into the measurements as much as possible
- At the same time, allowing for combination of the measurements between different decay channels as well as different experiments
- Evolved from stage 0 to the-present stage 1.2

First categorization step

- VBF-2jet-tagged
- VH-hadronic-tagged
- VH-leptonic-tagged
- $\mathrm{t}\bar{t}\mathrm{H}$-hadronic-tagged
- $\mathrm{t}\bar{t}\mathrm{H}$-leptonic-tagged
- VBF-1jet-tagged
- Untagged category for the remaining events

Each of these categories requires certain number of jets and/or leptons in the final state. Additionally, they have certain constraint on their respective kinematic discriminant value.

In the second categorization step, they use stage 1.2 of STXS framework followed by merging of bins to finally obtain 22 reconstructed event categories (higher granularity).

Reconstructed event category	1st categorization step	Number of jets	Kinematical requirements (GeV)	Targeted production bin
Untagged-0j-$p_{\mathrm{T}}^{4\ell}[0,10]$	Untagged	0	$0 < p_{\mathrm{T}}^{4\ell} < 10$	$\mathtt{ggH\text{-}0j/p_T}[0,10]$
Untagged-0j-$p_{\mathrm{T}}^{4\ell}[10,200]$	Untagged	0	$10 < p_{\mathrm{T}}^{4\ell} < 200$	$\mathtt{ggH\text{-}0j/p_T}[10,200]$
Untagged-1j-$p_{\mathrm{T}}^{4\ell}[0,60]$	Untagged	1	$0 < p_{\mathrm{T}}^{4\ell} < 60$	$\mathtt{ggH\text{-}1j/p_T}[0,60]$
Untagged-1j-$p_{\mathrm{T}}^{4\ell}[60,120]$	Untagged	1	$60 < p_{\mathrm{T}}^{4\ell} < 120$	$\mathtt{ggH\text{-}1j/p_T}[60,120]$
Untagged-1j-$p_{\mathrm{T}}^{4\ell}[120,200]$	Untagged	1	$120 < p_{\mathrm{T}}^{4\ell} < 200$	$\mathtt{ggH\text{-}1j/p_T}[120,200]$
Untagged-2j-$p_{\mathrm{T}}^{4\ell}[0,60]$	Untagged	2	$0 < p_{\mathrm{T}}^{4\ell} < 60, m_{\mathrm{jj}} < 350$	$\mathtt{ggH\text{-}2j/p_T}[0,60]$
Untagged-2j-$p_{\mathrm{T}}^{4\ell}[60,120]$	Untagged	2	$60 < p_{\mathrm{T}}^{4\ell} < 120, m_{\mathrm{jj}} < 350$	$\mathtt{ggH\text{-}2j/p_T}[60,120]$
Untagged-2j-$p_{\mathrm{T}}^{4\ell}[120,200]$	Untagged	2	$120 < p_{\mathrm{T}}^{4\ell} < 200, m_{\mathrm{jj}} < 350$	$\mathtt{ggH\text{-}2j/p_T}[120,200]$
Untagged-$p_{\mathrm{T}}^{4\ell} > 200$	Untagged	—	$p_{\mathrm{T}}^{4\ell} > 200$	$\mathtt{ggH/p_T} > 200$
Untagged-2j-$m_{\mathrm{jj}} > 350$	Untagged	2	$m_{\mathrm{jj}} > 350$	$\mathtt{ggH\text{-}2j/m_{jj}} > 350$
VBF-1jet-tagged	VBF-1jet-tagged	—	—	`qqH-rest`
VBF-2jet-tagged-$m_{\mathrm{jj}}[350,700]$	VBF-2jet-tagged	—	$p_{\mathrm{T}}^{4\ell} < 200, p_{\mathrm{T}}^{4\ell\mathrm{jj}} < 25, 350 < m_{\mathrm{jj}} < 700$	$\mathtt{qqH\text{-}2j/m_{jj}}[350,700]$
VBF-2jet-tagged-$m_{\mathrm{jj}} > 700$	VBF-2jet-tagged	—	$p_{\mathrm{T}}^{4\ell} < 200, p_{\mathrm{T}}^{4\ell\mathrm{jj}} < 25, m_{\mathrm{jj}} > 700$	$\mathtt{qqH\text{-}2j/m_{jj}} > 700$
VBF-3jet-tagged-$m_{\mathrm{jj}} > 350$	VBF-2jet-tagged	—	$p_{\mathrm{T}}^{4\ell} < 200, p_{\mathrm{T}}^{4\ell\mathrm{jj}} > 25, m_{\mathrm{jj}} > 350$	$\mathtt{qqH\text{-}3j/m_{jj}} > 350$
VBF-2jet-tagged-$p_{\mathrm{T}}^{4\ell} > 200$	VBF-2jet-tagged	—	$p_{\mathrm{T}}^{4\ell} > 200, m_{\mathrm{jj}} > 350$	$\mathtt{qqH\text{-}2j/p_T} > 200$
VBF-rest	VBF-2jet-tagged	—	$m_{\mathrm{jj}} < 350$	`qqH-rest`
VH-hadronic-tagged-$m_{\mathrm{jj}}[60,120]$	VH-hadronic-tagged	—	$60 < m_{\mathrm{jj}} < 120$	$\mathtt{qqH\text{-}2j/m_{jj}}[60,120]$
VH-rest	VH-hadronic-tagged	—	$m_{\mathrm{jj}} < 60$ or $m_{\mathrm{jj}} > 120$	`qqH-rest`
VH-leptonic-tagged-$p_{\mathrm{T}}^{4\ell}[0,150]$	VH-leptonic-tagged	—	$p_{\mathrm{T}}^{4\ell} < 150$	$\mathtt{VH\text{-}lep/p_T^H}[0,150]$
VH-leptonic-tagged-$p_{\mathrm{T}}^{4\ell} > 150$	VH-leptonic-tagged	—	$p_{\mathrm{T}}^{4\ell} > 150$	$\mathtt{VH\text{-}lep/p_T^H} > 150$
$\mathrm{t\bar{t}H}$-leptonic-tagged	$\mathrm{t\bar{t}H}$-leptonic-tagged	—	—	`ttH`
$\mathrm{t\bar{t}H}$-hadronic-tagged	$\mathrm{t\bar{t}H}$-hadronic-tagged	—	—	`ttH`

Figure 2: Event categorization criteria targeting stage 1.2 STXS production bins

Results!

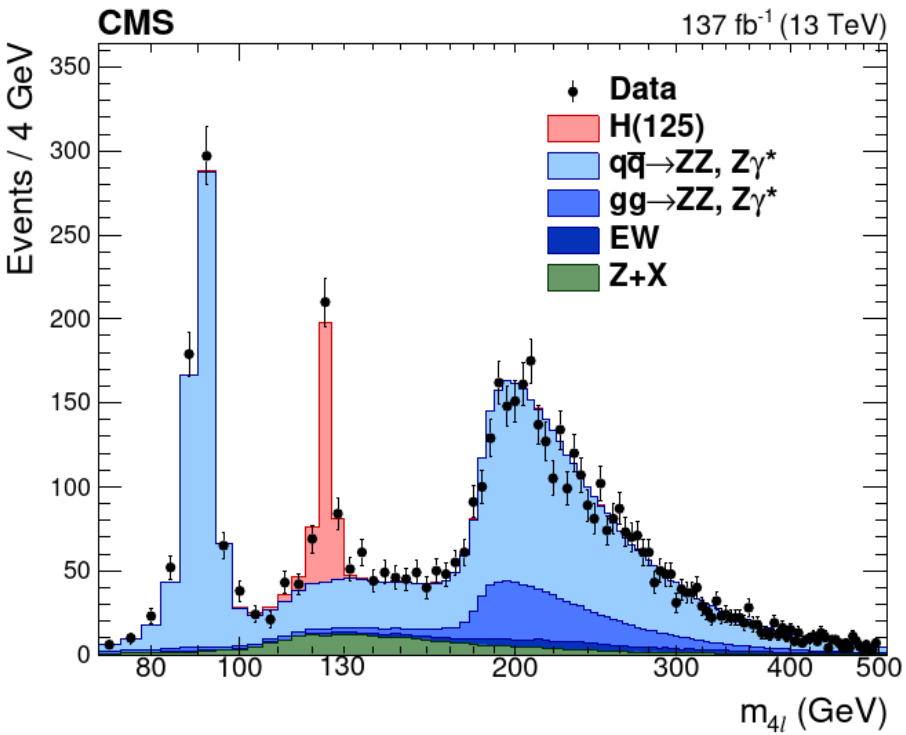

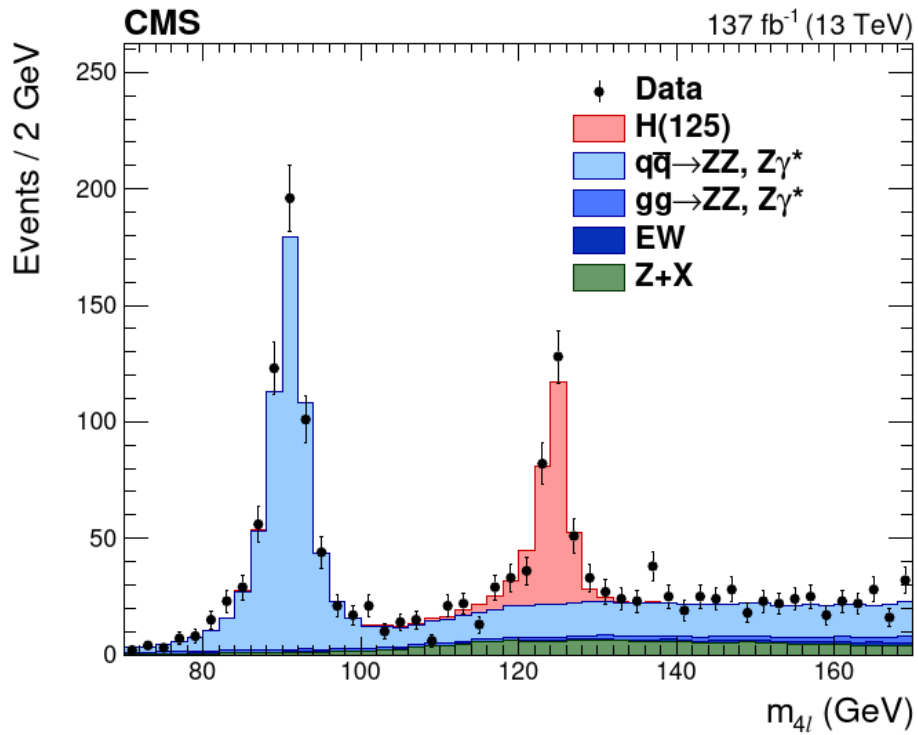

Figure 3: Four-lepton mass distribution

- For 4e, 4μ, 2e2μ events together
- Error bars correspond to intervals of 68% confidence interval
- ZZ and rare electroweak backgrounds normalized to SM expectation
- Z+X background to the estimation from data

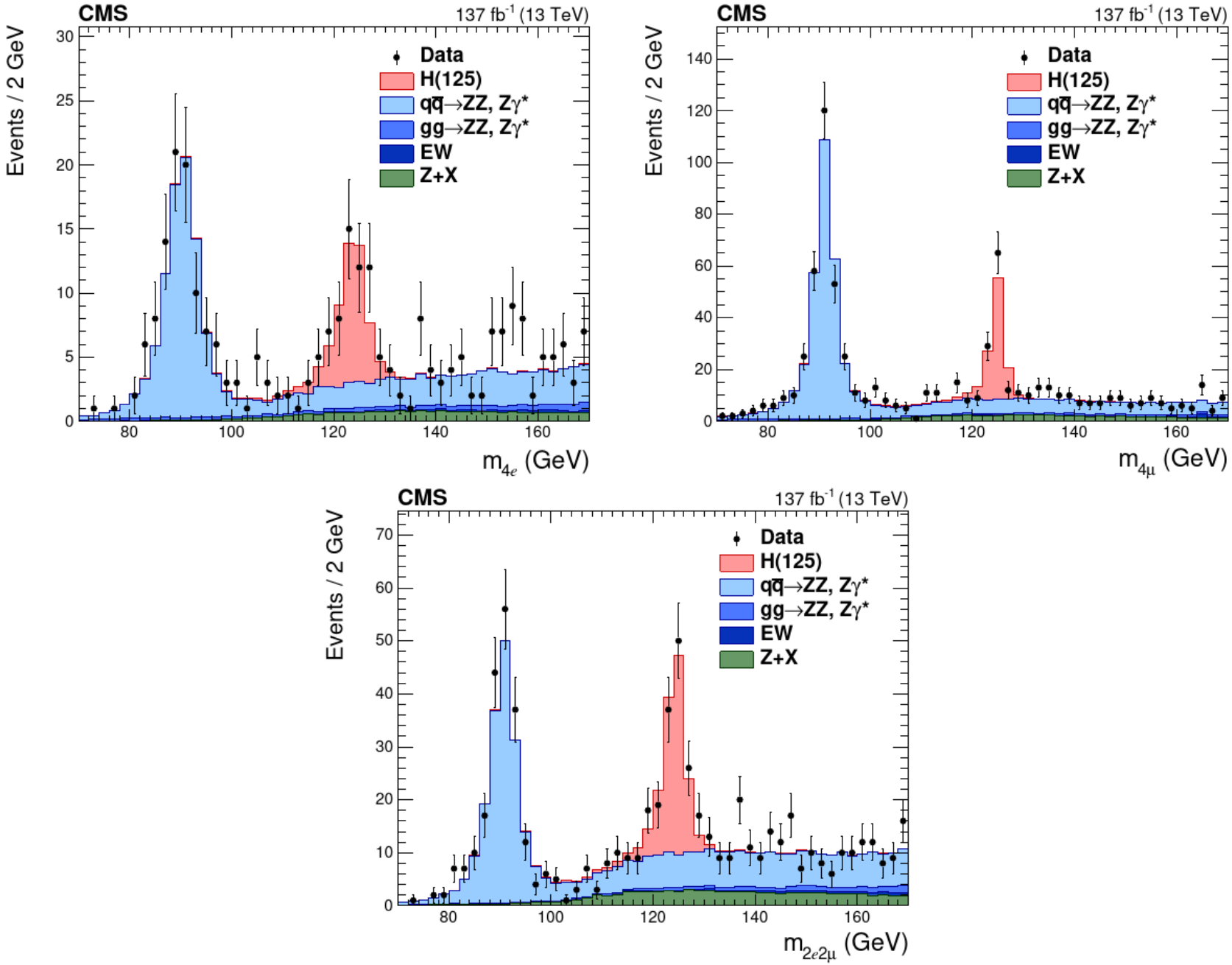

Figure 4: Four-lepton mass distribution; 4e(upper left), 4μ(upper right), 2e2μ(lower)

Reconstructed event category	Signal							Background				Expected		Observed
	ggH	VBF	WH	ZH	$t\bar{t}H$	$b\bar{b}H$	q_tH	$q\bar{q} \to ZZ$	$gg \to ZZ$	EW	Z+X	signal	total	
Untagged-0j-$p_T^{4\ell}[0,10]$	27.7	0.09	0.03	0.03	0.00	0.15	0.00	71.5	3.06	0.01	3.21	27.9±0.1	106±0	114
Untagged-0j-$p_T^{4\ell}[10,200]$	96.2	1.69	0.60	0.77	0.01	1.01	0.00	98.1	11.6	0.35	37.8	100±0	248±1	278
Untagged-1j-$p_T^{4\ell}[0,60]$	26.8	1.51	0.56	0.48	0.01	0.45	0.01	25.3	3.02	0.64	14.2	29.8±0.1	72.9±0.4	74
Untagged-1j-$p_T^{4\ell}[60,120]$	13.5	1.31	0.51	0.41	0.02	0.11	0.01	7.81	0.82	0.62	7.95	15.9±0.1	33.1±0.3	20
Untagged-1j-$p_T^{4\ell}[120,200]$	3.51	0.60	0.17	0.17	0.01	0.02	0.00	1.15	0.19	0.25	1.63	4.48±0.05	7.69±0.16	11
Untagged-2j-$p_T^{4\ell}[0,60]$	3.45	0.29	0.15	0.14	0.08	0.09	0.02	2.14	0.32	0.63	4.75	4.20±0.06	12.1±0.2	14
Untagged-2j-$p_T^{4\ell}[60,120]$	5.26	0.56	0.24	0.19	0.12	0.04	0.03	2.19	0.30	0.72	4.14	6.43±0.06	13.8±0.2	15
Untagged-2j-$p_T^{4\ell}[120,200]$	3.07	0.40	0.16	0.13	0.07	0.01	0.02	0.75	0.14	0.34	1.19	3.86±0.05	6.28±0.14	7
Untagged-$p_T^{4\ell} > 200$	2.79	0.62	0.21	0.17	0.07	0.01	0.02	0.43	0.21	0.21	0.73	3.89±0.04	5.47±0.11	3
Untagged-2j-$m_{jj} > 350$	0.77	0.16	0.06	0.04	0.05	0.01	0.01	0.34	0.06	0.31	1.71	1.12±0.02	3.54±0.14	3
VBF-1jet-tagged	15.5	3.29	0.22	0.16	0.00	0.13	0.01	6.85	1.53	0.20	2.44	19.3±0.1	30.3±0.2	27
VBF-2jet-tagged-$m_{jj}[350,700]$	0.83	1.19	0.01	0.01	0.00	0.01	0.00	0.19	0.07	0.11	0.14	2.05±0.03	2.55±0.05	2
VBF-2jet-tagged-$m_{jj} > 700$	0.43	1.96	0.00	0.00	0.00	0.00	0.00	0.07	0.05	0.12	0.03	2.40±0.02	2.67±0.03	1
VBF-3jet-tagged-$m_{jj} > 350$	2.52	2.35	0.06	0.06	0.03	0.03	0.05	0.62	0.21	0.64	2.43	5.11±0.05	9.01±0.17	12
VBF-2jet-tagged-$p_T^{4\ell} > 200$	0.44	0.79	0.01	0.01	0.01	0.00	0.01	0.03	0.03	0.04	0.06	1.26±0.02	1.42±0.03	0
VBF-rest	2.48	0.94	0.13	0.09	0.04	0.04	0.01	0.98	0.20	0.39	2.18	3.74±0.05	7.49±0.17	5
VH-hadronic-tagged-$m_{jj}[60,120]$	4.11	0.25	1.09	0.96	0.13	0.06	0.02	1.69	0.22	0.52	2.93	6.62±0.06	12.0±0.2	12
VH-rest	0.57	0.03	0.09	0.06	0.03	0.01	0.00	0.16	0.02	0.06	0.33	0.79±0.02	1.36±0.06	0
VH-leptonic-tagged-$p_T^{4\ell}[0,150]$	0.33	0.04	0.85	0.26	0.10	0.03	0.03	2.16	0.36	0.19	1.11	1.64±0.02	5.47±0.13	10
VH-leptonic-tagged-$p_T^{4\ell} > 150$	0.02	0.01	0.21	0.06	0.04	0.00	0.01	0.05	0.01	0.03	0.08	0.35±0.01	0.52±0.03	0
$t\bar{t}H$-leptonic-tagged	0.02	0.01	0.02	0.02	0.68	0.00	0.03	0.08	0.01	0.23	0.21	0.79±0.01	1.32±0.07	0
$t\bar{t}H$-hadronic-tagged	0.18	0.05	0.03	0.05	0.86	0.01	0.03	0.03	0.01	0.82	1.06	1.22±0.01	3.15±0.14	2

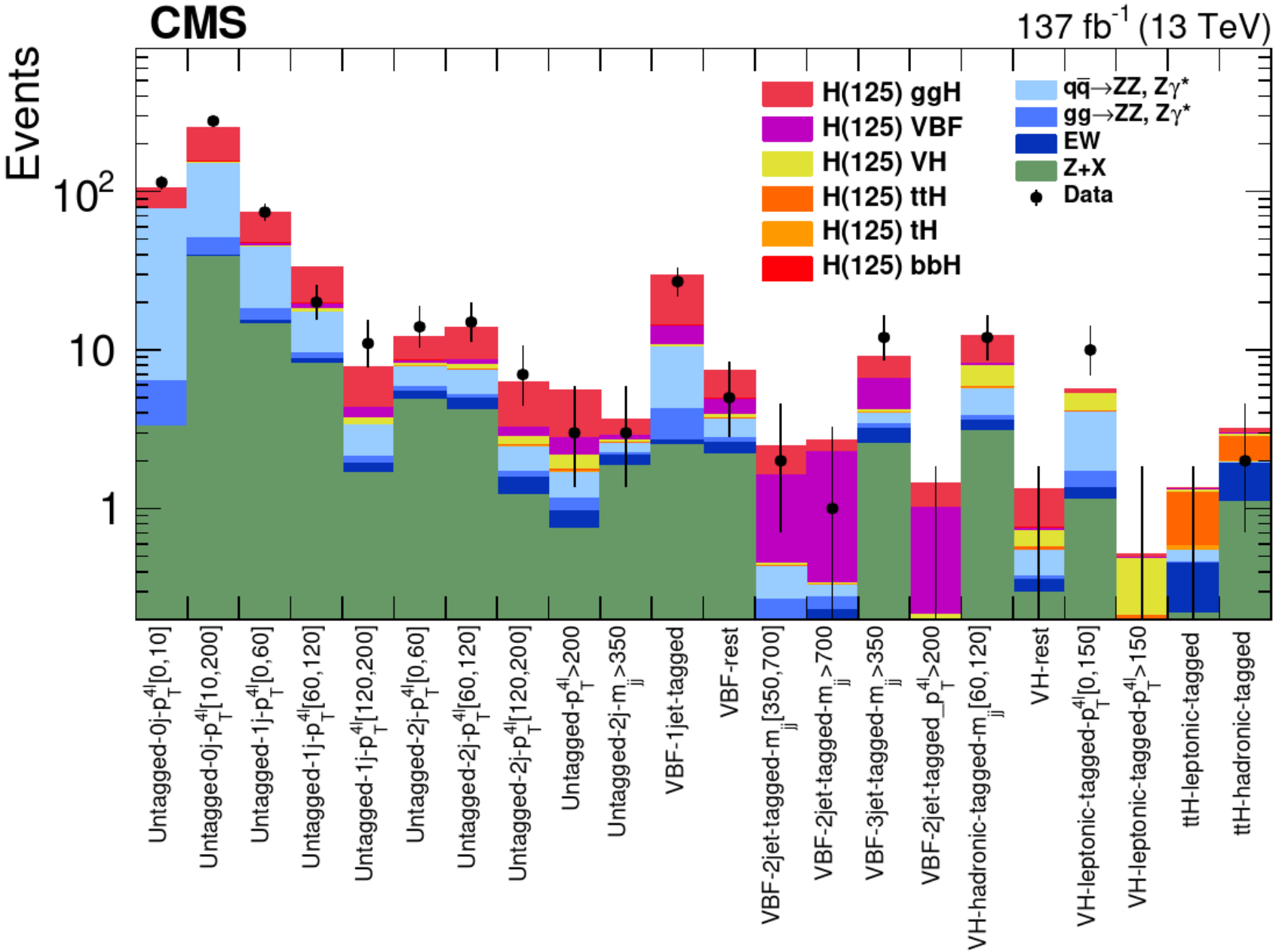

Figure 5: Distribution of the expected and observed number of events for the reconstructed event categories

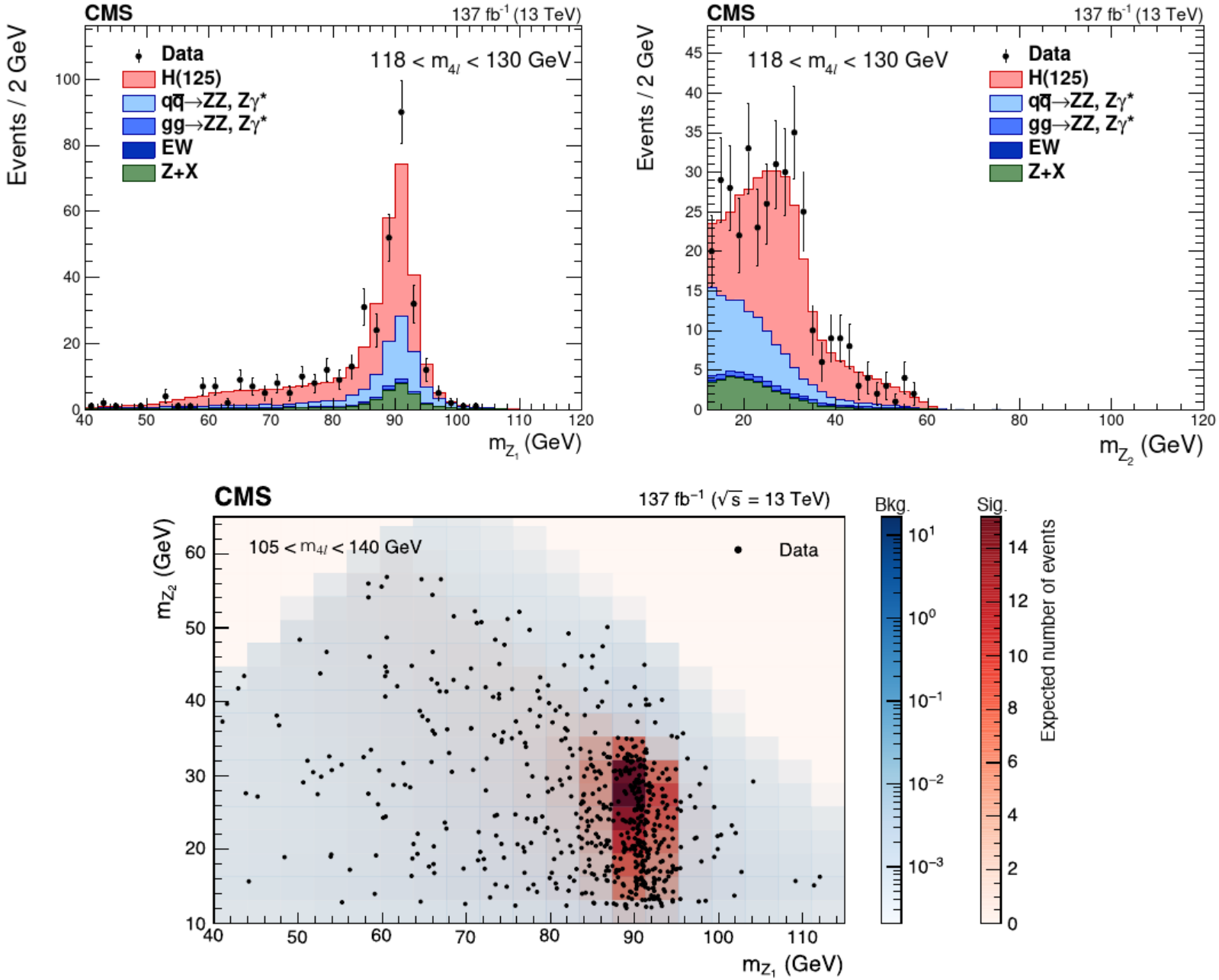

Figure 6: Distribution of the reconstructed Z1 and Z2

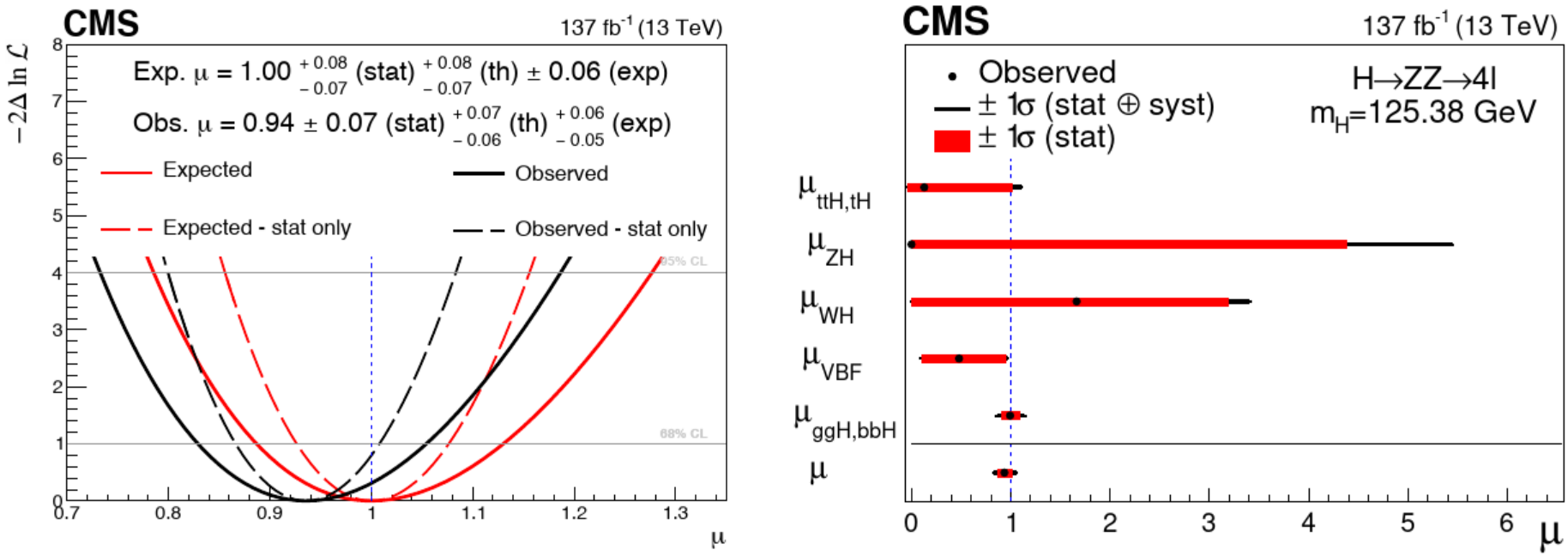

Figure 7: Likelihood vs Signal strength from the analysis

	Expected	Observed
$\mu_{t\bar{t}H,q_tH}$	$1.00^{+1.23}_{-0.77}\,(\text{stat})^{+0.51}_{-0.06}\,(\text{syst})$	$0.17^{+0.88}_{-0.17}\,(\text{stat})^{+0.42}_{-0.00}\,(\text{syst})$
μ_{WH}	$1.00^{+1.83}_{-1.00}\,(\text{stat})^{+0.75}_{-0.00}\,(\text{syst})$	$1.66^{+1.52}_{-1.66}\,(\text{stat})^{+0.85}_{-0.00}\,(\text{syst})$
μ_{ZH}	$1.00^{+4.79}_{-1.00}\,(\text{stat})^{+6.76}_{-0.00}\,(\text{syst})$	$0.00^{+4.38}_{-0.00}\,(\text{stat})^{+3.24}_{-0.00}\,(\text{syst})$
μ_{VBF}	$1.00^{+0.53}_{-0.44}\,(\text{stat})^{+0.18}_{-0.12}\,(\text{syst})$	$0.48^{+0.46}_{-0.37}\,(\text{stat})^{+0.14}_{-0.10}\,(\text{syst})$
$\mu_{ggH,b\bar{b}H}$	$1.00 \pm 0.10\,(\text{stat})^{+0.12}_{-0.10}\,(\text{syst})$	$0.99 \pm 0.09\,(\text{stat})^{+0.11}_{-0.09}\,(\text{syst})$
μ	$1.00^{+0.08}_{-0.07}\,(\text{stat})^{+0.10}_{-0.08}\,(\text{syst})$	$0.94 \pm 0.07\,(\text{stat})^{+0.09}_{-0.08}\,(\text{syst})$

Figure 8: Signal strength

	$(\sigma\mathcal{B})_{\text{obs}}$ (fb)	$(\sigma\mathcal{B})_{\text{SM}}$ (fb)	$(\sigma\mathcal{B})_{\text{obs}}/(\sigma\mathcal{B})_{\text{SM}}$
ttH	3^{+16}_{-3}	15.9 ± 1.4	$0.16^{+0.98}_{-0.16}$
VH-lep	41^{+52}_{-35}	25.9 ± 0.8	$1.56^{+1.99}_{-1.34}$
qqH	61^{+53}_{-44}	122 ± 6	$0.50^{+0.44}_{-0.36}$
ggH	1214^{+135}_{-125}	1192 ± 95	$1.02^{+0.11}_{-0.10}$
Inclusive	1318^{+130}_{-122}	1369 ± 164	$0.96^{+0.10}_{-0.09}$

Figure 9: Measured product of cross sections and branching fraction

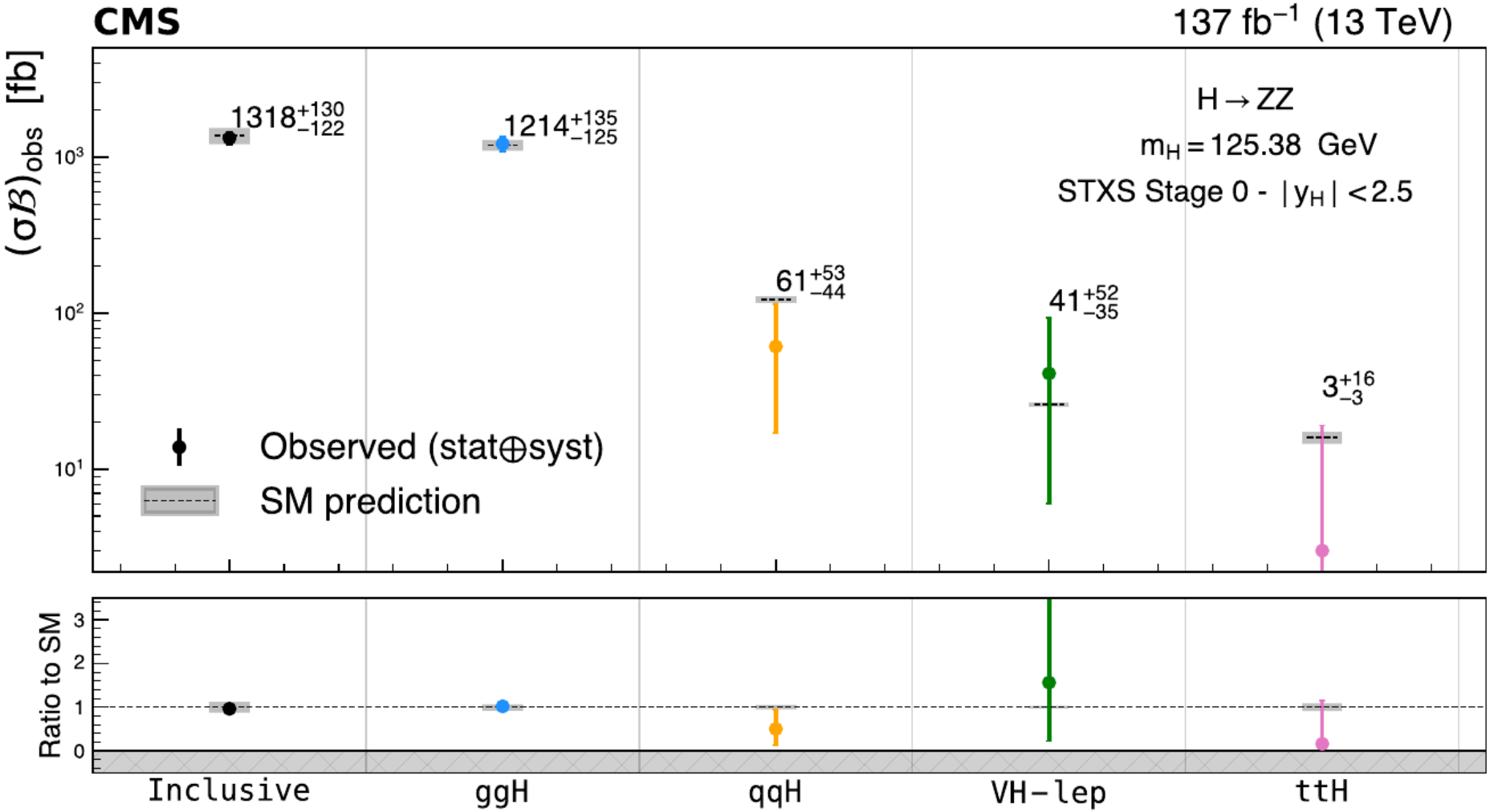

Figure 10: Plot of measured product of cross sections and branching fraction in first categorization step

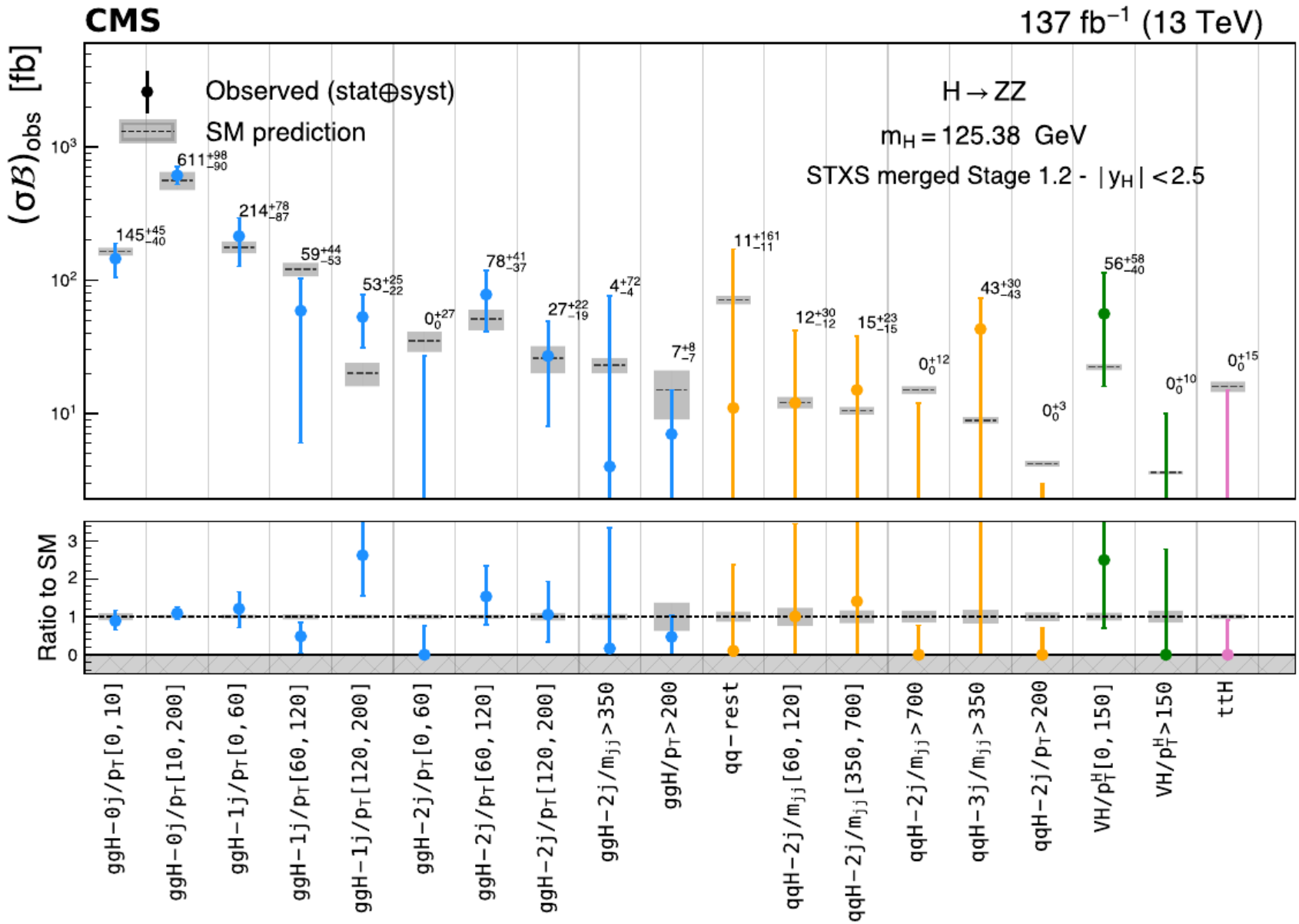

Figure 11: Plot of measured product of cross sections and branching fraction after using STXS framework

	2e2μ (fb)	4μ (fb)	4e (fb)	Inclusive (fb)
2016	$1.22^{+0.38}_{-0.30}$	$0.89^{+0.22}_{-0.19}$	$1.07^{+0.44}_{-0.33}$	$3.19^{+0.68}_{-0.56} = 3.19^{+0.48}_{-0.45}\,(\text{stat})^{+0.48}_{-0.33}\,(\text{syst})$
2017	$1.64^{+0.41}_{-0.35}$	$0.82^{+0.21}_{-0.18}$	$0.56^{+0.29}_{-0.22}$	$3.01^{+0.60}_{-0.50} = 3.01^{+0.44}_{-0.41}\,(\text{stat})^{+0.41}_{-0.27}\,(\text{syst})$
2018	$1.17^{+0.27}_{-0.24}$	$0.66^{+0.15}_{-0.13}$	$0.73^{+0.24}_{-0.20}$	$2.57^{+0.42}_{-0.38} = 2.57^{+0.33}_{-0.31}\,(\text{stat})^{+0.27}_{-0.23}\,(\text{syst})$
2016–2018	$1.31^{+0.20}_{-0.19}$	$0.78^{+0.10}_{-0.10}$	$0.76^{+0.18}_{-0.16}$	$2.84^{+0.34}_{-0.31} = 2.84^{+0.23}_{-0.22}\,(\text{stat})^{+0.26}_{-0.21}\,(\text{syst})$

Figure 12: Inclusive fiducial cross section

Bin range (GeV)	$d\sigma_{fid}$ (fb)	unc.	(stat)	(syst)
0–10	0.32	$^{+0.11}_{-0.10}$	$^{+0.10}_{-0.09}$	$^{+0.04}_{-0.03}$
10–20	0.67	$^{+0.14}_{-0.13}$	$^{+0.13}_{-0.12}$	$^{+0.06}_{-0.05}$
20–30	0.41	$^{+0.12}_{-0.10}$	$^{+0.11}_{-0.10}$	$^{+0.04}_{-0.04}$
30–45	0.51	$^{+0.12}_{-0.10}$	$^{+0.11}_{-0.10}$	$^{+0.04}_{-0.04}$
45–80	0.45	$^{+0.10}_{-0.09}$	$^{+0.10}_{-0.09}$	$^{+0.04}_{-0.03}$
80–120	0.30	$^{+0.08}_{-0.07}$	$^{+0.07}_{-0.07}$	$^{+0.02}_{-0.02}$
120–200	0.19	$^{+0.06}_{-0.05}$	$^{+0.06}_{-0.05}$	$^{+0.01}_{-0.01}$
200–13000	0.03	$^{+0.02}_{-0.02}$	$^{+0.02}_{-0.01}$	$^{+0.00}_{-0.00}$

Figure 13: Differential fiducial cross section with bins at fixed Higgs mass of 125.38 GeV

Conclusions

- Using data samples from an integrated luminosity of $137\,\text{fb}^{-1}$, several measurements of the Higgs boson production in the four-lepton final state
- Measured signal strength modifier,
$$\boxed{\mu = 0.94 \pm 0.07(\text{stat})^{+0.07}_{-0.06}(\text{theo})^{+0.06}_{-0.05}(\text{exp})}$$
- Integrated fiducial cross section, $\boxed{\sigma_{\text{fid}} = 2.84^{+0.23}_{-0.22}(\text{stat})^{+0.26}_{-0.21}(\text{syst})\,\text{fb}}$ is compatible with the standard model prediction of $2.84 \pm 0.15\,\text{fb}$
- New set of measurements designed to quantify Higgs production in specific kinematical regions of phase space
- Differential cross section as a function of transverse momentum, rapidity of Higgs, associated jets are determined

The condensed takeaway

All rules are consistent, within their uncertainties, with the expectations for the standard model Higgs boson.